FUSE Observation of the Ultramassive White Dwarf PG 1658+441

Jean Dupuis, Pierre Chayer[1]

Department of Physics and Astronomy, The Johns Hopkins University, Baltimore, MD 21218

jdupuis@pha.jhu.edu, chayer@pha.jhu.edu

Stéphane Vennes

Department of Mathematics, Australian National University, Canberra, Australia ACT0200

vennes@wintermute.anu.edu.au

and

Nicole F. Allard[2], Guillaume Hébrard

Institut d'Astrophysique de Paris, F-75014 Paris, France

allard@iap.fr, hebrard@iap.fr

ABSTRACT

We present an analysis of the *Far Ultraviolet Spectroscopic Explorer* (*FUSE*) spectrum of the ultramassive ($M = 1.31$ M$_\odot$), magnetic ($B_s = 2.3$ MG) white dwarf PG 1658+441. The far ultraviolet (FUV) spectrum exhibits very broad Lyman lines and quasi-molecular Lyman β satellites, but weak Lyman γ satellites may also be present. PG 1658+441 is the hottest white dwarf known to show these satellite features. We fit the Lyman lines with stellar models and obtain atmospheric parameters consistent with a published analysis of the Balmer lines. By averaging results obtained for the different *FUSE* segments, we determine $T_{\rm eff} = 29,620 \pm 500$ K and $\log g = 9.31 \pm 0.07$. The models match the data over large portions of the spectrum but discrepancies remain near the satellite features. Finally, no trace elements have been identified in the FUV spectrum, and we provide abundance upper limits for C, N, Si, and P.

[1]also with the Department of Physics and Astronomy, University of Victoria, PO Box 3055, Station Csc, Victoria, BC V8W 3P6, Canada.

[2]also with Observatoire de Paris-Meudon, LERMA, F-92195 Meudon Principal Cedex, France.

Subject headings: line: profiles — stars: abundances — stars: individual (PG 1658+441) — stars: ultraviolet — white dwarfs

1. Introduction

The DA white dwarf PG 1658+441 was discovered in the Palomar-Green survey (Green et al. 1986). Liebert et al. (1983) announced the presence of a magnetic field in this white dwarf and presented a detailed analysis of the energy distribution consistent with a 30,000 K pure hydrogen star. They measured a mean surface field of $B_s = 2.3$ MG from the Zeeman splitting of the Balmer lines. The magnetic field of PG 1658+441 was studied in detail by Achilleos & Wickramasinghe (1989) using offset magnetic dipole models. They measured a field of $B_d = 3.0 \pm 0.5$ MG with a viewing angle between 40° and 50°. Schmidt et al. (1992) reported the first surface gravity measurement by fitting the Balmer line profiles with synthetic profiles including Zeeman splitting. They reached the surprising conclusion that PG 1658+441 has an abnormally high surface gravity of $\log g = 9.36 \pm 0.07$ corresponding to a stellar mass of 1.31 ± 0.02 $M_\odot$. The mass of PG 1658+441 appears much higher than the average mass of field white dwarfs ($\approx 0.55 - 0.60 M_\odot$). While searching for helium in ultramassive white dwarfs, Dupuis et al. (2002) analyzed the *EUVE* spectrum of PG 1658+441 and found evidence for a small quantity of atmospheric contaminants which was assumed to be helium.

The origin of PG 1658+441 and, more generally, of the population of hot ultramassive white dwarfs discovered in recent EUV/soft X-ray surveys is yet unknown. These objects appear to form a secondary peak in the white dwarf mass distribution near 1.25 $M_\odot$ and a substantial fraction of these objects are also magnetic (Vennes 1999). As recently discussed by Dupuis et al. (2002), the problem posed with the mass of these stars is that they exceed the maximum mass of a C/O core ($\approx 1.1 M_\odot$) formed by the evolution of intermediate mass stars (Weidemann 2000). While it is not unconceivable to form white dwarfs with O/Ne core with mass exceeding 1.1 $M_\odot$ through single star evolution channels (Nomoto 1984; Garcia-Berro et al. 1997), Schmidt et al. (1992) raised the issue that if PG1658+441 originates from a star with a mass in excess of 6–8 $M_\odot$, it should be relatively young and would be likely associated with a stellar cluster. Because PG1658+441 is not an obvious member of any cluster, Schmidt et al. (1992) proposed instead that PG1658+441 could be the product of the coalescence of a double-degenerate system. Such a system is expected to rotate rapidly and show photometric or magnetic field variability, but there is no evidence yet that PG1658+441 is variable (Liebert et al. 1983; Shtol' et al. 1997). There is also the possibility that PG1658+441 originates from an older Ap star, and that a peculiar initial-

mass to final-mass relation applies to the evolution of magnetic stars.

Why observe ultramassive white dwarfs with *FUSE*? Atmospheric parameters are usually obtained from a model atmosphere analysis of Balmer line profiles. With recent advance in FUV astronomy, spectroscopy of the hydrogen Lyman series has been made possible, and an independent diagnostic of atmospheric properties of hot white dwarfs is now available (see for example Finley et al. 1997, Barstow et al. 2001, and Barstow et al. 2003). The Lyman line series also allows for a test of line broadening theory in the high density conditions encountered in the atmosphere of ultramassive white dwarfs. The high spectral resolution ($R = 17000 - 20000$) achieved with *FUSE* allows for the detection of heavy element lines and helps better characterize the atmospheric composition of ultramassive white dwarfs. The detection of helium in the *EUVE* spectrum of GD 50 by Vennes et al. (1996) indicates that trace elements may be present in ultramassive white dwarf atmospheres. Although a study by Dupuis et al. (2002) shows that GD 50 is quite unique, the case is still open due to the limited sensitivity of *EUVE*. *FUSE* observations of this class of objects are needed to provide an independent determination of their stellar parameters.

We present an analysis of the *FUSE* spectrum of the ultramassive white dwarf PG 1658+441. In section 2, we describe the observations and data reduction. In section 3, we present the model atmosphere analysis and describe the abundance measurements of C, N, Si, and P. We also analyze the Lyman line profiles which clearly show the quasi-molecular satellite features of H_2^+ in the wings of Lyman-β and Lyman-γ. This result is interesting in view of the high surface gravity and relatively high effective temperature of the star. We conclude by discussing the implications of our results on the origin of ultramassive white dwarfs and we summarize our findings.

2. Observations and Data Reduction

PG 1658+441 was observed as part of our *FUSE* Cycle 2 GI program B122. The spacecraft and the instruments are described in Moos et al. (2000, 2002) and an initial account of the calibration is given in Sahnow et al. (2000). *FUSE* provides spectra from 905 to 1187 Å with a velocity resolution of 15–20 km s^{-1} in four independent channels (SiC1, SiC2, LiF1, LiF2) each split in two segments (A and B). The sequence of 16 exposures was initiated on 17 July 2001 at 13:42:45 (UT) for a total exposure time of 28483 seconds. The target was centered in the LWRS aperture and the observations were made in TTAG mode. We have reprocessed the data with CALFUSE version 2.2.2. We found the target to be out of the aperture during 4 out of the 16 exposures in the LiF2 channel.

We have coadded the spectra of each channel from all exposures making sure we selected only photometric exposures. The coaddition is made using the program "cf_combine" provided with CALFUSE. Figures 1 and 2 show the combined spectra binned by 24 pixels for each segment of the *FUSE* spectrometer. The Lyman lines series from the white dwarf photosphere clearly dominate the spectrum. A broad depression centered on 1150 Å was initially evident in the LiF1B spectrum, but it was not observed in the LiF2A spectrum which covers a similar wavelength range. This instrumental artifact, nicknamed the "worm", is thought to be due to blockage of the spectral image by a grid wire above the surface of the micro-channel plate detector. We have derived a "worm" correction using the LiF2A segment as a reference spectrum. We smoothed the ratio of the LiF2A to LiF1B spectra using cubic splines and corrected the LiF1B spectrum by multiplying it by this smoothed ratio.

3. Analysis of the FUV spectrum of PG 1658+441

In order to analyze the spectrum of PG 1658+441, we used the model atmosphere code TLUSTY(v. 195) (Hubeny 1988; Hubeny & Lanz 1995) and the spectral synthesis code SYNSPEC version 45 (SYNSPEC45) which incorporates hydrogen Lyman line opacities (Lemke 1997), and SYNSPEC version 48 (SYNSPEC48) which incorporates new quasi-molecular satellite line opacities of H_2 and H_2^+ computed by N. Allard for Lyman-α, Lyman-β, and Lyman-γ. The quasi-molecular opacity tables of Lyman-β were specifically recomputed for a temperature of 30,000 K, more appropriate for PG 1658+441. The general method is described by Allard et al. (1998) who computed theoretical line profiles for Lyman-β including quasi-molecular satellites due to H_2^+ with a variable dipole.

3.1. Quasi-Molecular Satellites

First, we computed a pure hydrogen model atmosphere in non-LTE adopting published atmospheric parameters of PG 1658+441, $T_{\rm eff} = 30510 \pm 200$K and $\log g = 9.36 \pm 0.07$ (Schmidt et al. 1992). Next, we calculated a synthetic spectrum using SYNSPEC45 and covering the *FUSE* spectral range. This generic model is normalized to match the absolute flux level in LiF1A and LiF1B. The normalization corresponds to a V magnitude of about 14.79 and agrees with the same normalization based on *International Ultraviolet Explorer* spectra (Dupuis et al. 2002).

Figures 1 and 2 show a comparison between the model spectrum (*solid lines*) and the

FUSE spectra. The generic model seems in good agreement with the observed line profiles, even though we have not yet attempted a formal fit of the Lyman line profiles at this point (see section 3.2). However, a closer inspection of Figures 1 and 2 shows discrepancies in the Lyman-β and Lyman-γ red wings.

Broad absorption troughs are apparent at 1058 Å and 1076 Å in the red wing of Lyman-β of the LiF1A, LiF2B, SiC1A, and SiC2B spectra. The troughs are attributed to H_2^+ quasi-molecular satellite features previously detected in cooler white dwarfs by the *Hopkins Ultraviolet Telescope* (*HUT*) (Koester et al. 1996), *ORFEUS* (Koester et al. 1998), and *FUSE* (Wolff et al. 2001; Hébrard et al. 2002). In addition, the features possibly present on the red wing of Lyman-γ do correspond to quasi-molecular features detected in the *HUT* spectra of WD1031−114 and WD0644+375 by Koester et al. (1998) and in the *FUSE* spectrum of CD−38^{o}10980 by Wolff et al. (2001) and included for the first time in model comparisons presented by Hébrard et al. (2003). PG 1658+441 is the hottest white dwarf so far to show these FUV spectral features.

The validity of the Balmer and Lyman line profiles is questionable because in high-gravity stars the Lyman line wings form at depths where the electronic density is between $10^{17} - 10^{18}$ cm^{-3}, near the limit of Lemke's tables (Lemke 1997). Moreover, the tables should not be applied directly to PG 1658+441 because they do not include the satellite lines from quasi-molecules of H_2^+, but the good agreement between the synthetic spectra and the observations (Figs. 1 and 2) away from the quasi-molecular satellite features suggests that they are a good approximation.

The emergence of quasi-molecular satellite lines of H_2^+ in PG 1658+441 is possibly due to its high surface gravity which implies larger particle densities in the line forming region. Because PG 1658+441 is hot, hydrogen should be more ionized but the high surface gravity implies larger pressures (or larger electronic densities) in the atmosphere which in turn favor recombination. Because of this effect, we find the number density of shydrogen atoms to be comparable with the one found in the atmospheres of DA in which the quasi-molecular satellites lines have been previously detected. These stars are typically cooler with $T_{\rm eff}$ up to about 20,000K and less massive with $\log g$ close to 8. Because the quasi-molecular opacity is proportional to the proton and H I densities, we predict that the H_2^+ quasi-molecular satellite lines become apparent at higher effective temperatures in WD with larger surface gravities.

Finally, adopting the same effective temperature and surface gravity ($T_{\rm eff} = 30,510$ K, $\log g = 9.36$), we computed a synthetic spectrum using SYNSPEC48 which includes quasi-molecular satellite line opacities. Figures 1 and 2 show a comparison between the data and the synthetic spectra which include the quasi-molecular satellite lines of Lyman-β and Lyman-γ (*dashed lines*). The predicted satellite lines do not agree well with the data as

the H_2^+ satellites at 1058 Å and 1076 Å are somewhat too deep and shifted toward shorter wavelengths. On the other hand, the predicted Lyman-γ satellites are too weak. There is also a subtle kink predicted in the Lyman-β profile near 1037 Å which is possibly present in the data and better seen in Figure 3 (see next section). This preliminary comparison is certainly promising but we must investigate whether or not the agreement could be improved by doing a formal fit of the *FUSE* spectrum.

3.2. Atmospheric Parameters

To determine the atmospheric parameters more accurately, we have computed a fine grid of model atmospheres and synthetic spectra. The spectra were computed with SYNSPEC48 which includes the quasi-molecular opacities of H_2^+ for Lyman-β and Lyman-γ. The grid, appropriate for determining the atmospheric parameters of PG 1658+441, includes effective temperatures from 25,000 to 35,000K in steps of 1000K and surface gravities from 7.5 to 9.5 ($\log g$) in steps of 0.1 dex.

Each of the spectroscopic channels showing the Lyman lines are fitted separately so that we obtain independent measurements of the stellar parameters. We used a χ^2–minimization technique to find the best-fit parameters, $T_{\rm eff}$ and $\log g$. We excluded regions contaminated by airglow, interstellar absorption lines, as well as detector edges where the spectra are of poor quality. We neglected Zeeman splitting which could produce shifts of the order of 1 Å or less in the core of Lyman-β and higher Lyman lines. The approximation does not affect the results because the line cores are already excluded from the fit. We also binned the spectra by 20 pixels (which corresponds to about 0.13Å) to improve the signal-to-noise ratio. For the fit of the Lyman-β line, we restrict the fit to wavelengths between 1005Å and 1050Å to exclude regions affected by the quasi-molecular satellites of Lyman-β and Lyman-γ. Including these regions had the consequence of driving the fits toward spurious solutions. The spectrum normalization (or scale factor) is also left as a free parameter in the fit. An overall wavelength shift of -0.4 Å was applied to the model spectra to align optimally the models with the data. Table 1 summarizes the results. The quoted error bars are computed from the projection of the $3-\sigma$ confidence contours in the $T_{\rm eff}$–$\log g$ plane. A representative example of a fit is shown on Figure 3 for the Lyman-β line in the LiF1A segment which shows how well the line is fitted up to where the quasi-molecular satellites become important.

As expected, there is some scatter in the parameter values derived from the different channels and segments which gives us an assessment of the systematic errors. The measured parameter values are consistent within the quoted error bars although the surface gravity measured from SiC2B appears to be greater. This last measurement is less reliable, as re-

flected by the larger error, because the Lyman-β profile from SiC2B is missing most of the blue wing (the wavelength coverage ends at 1017 Å). Minor differences observed between different channels are probably due to subtle flux calibration effects such as light blocking by grid wires or sensitivity degradation which are not perfectly accounted for in the data reduction. Nonetheless, the values obtained by taking the weighted mean of the six measurements are in agreement with those of Schmidt et al. (1992) although we seem to favor slightly lower values of the gravity and effective temperature.

Our results confirm the analysis of Schmidt et al. (1992) which was possibly affected by Zeeman splitting observed in the Balmer line cores. In general, they validate gravity measurements in low-field white dwarfs which are based on the modeling of spectral line wings computed at zero magnetic field. It is also interesting to note that Barstow et al. (2001) obtained a slightly lower value of the surface gravity based on the FUV *HUT* spectrum of the ultramassive white dwarf GD 50 compared to values based on optical spectra, but such differences do not appear worst than for less massive DA stars in their sample. Note that Friedrich et al. (1996) suggested that Stark broadening due to an electric field parallel to the magnetic field may be important in magnetic white dwarfs and that it may explain the broadness of PG 1658+441 Balmer lines. However, their best fit to an optical spectrum of PG 1658+441 is quite poor and may indicate that the effect is overestimated. We have not considered this effect.

3.3. Metal Abundance Upper Limits

A search for heavy elements in PG 1658+441 is motivated by the detection of helium in the atmosphere of GD 50 (Vennes et al. 1996) and by the possible detection of helium or other contaminants in the extreme-ultraviolet spectrum of PG 1658+441 (Dupuis et al. 2002). These observations suggest that other ultramassive white dwarfs may have some metals in their atmospheres. These metals may provide additional clues required to better understand the origin of these stars as they may be relics of the original composition of the ultramassive white dwarfs. Various scenarios for producing ultramassive white dwarfs predict hydrogen poor atmospheres. Therefore, it is important to understand the nature of ultramassive white dwarfs which appear to have hydrogen-rich atmospheres.

Thus, we have searched for the presence of metals in the atmosphere of PG 1658+441 but have found none of the usual suspects. Nevertheless, we have used the spectra to set upper limits on elements likely to be detected in *FUSE* spectra of white dwarfs, that is C, N, Si, and P. We computed non-LTE synthetic spectra for each element selected over a range of abundances varying from X/H = 10^{-9} to 10^{-5} in steps of 0.25 dex. The strongest predicted

lines (as shown on Fig. 4) are used to compute a 3–σ upper limit on the abundance. Note that the upper limits are measured at the rest wavelengths of the selected transitions, and that we corrected the wavelength scale for a predicted gravitational redshift of 211 km s^{-1}. There is an additional uncertainty related to our lack of knowledge of the radial velocity of PG 1658+441. Figure 4 shows the spectra on a velocity scale with $v = 0$ corresponding to the laboratory wavelength. The noise appears uniform over a range of ± 500 km s^{-1}. The linear Zeeman effect is not taken into account in the synthetic spectra, but it could shift the σ components by ± 360 km s^{-1} (assuming a surface average field of 2.3 MG). Limiting the analysis to the un-shifted component, this effect adds ≈ 0.5 dex to the abundance upper limits. However, the spectra do not show any evidence for shifted components. The results are shown in Figure 4 and summarized in Table 2. The upper limits are rather stringent and shows that PG 1658+441's atmosphere is metal poor and is consistent with having a pure hydrogen atmosphere.

4. Discussion and Summary

The fact that no trace elements are detected in the hydrogen atmosphere of PG 1658+441 is perhaps not so surprising. At such a high surface gravity we do not expect radiative acceleration to support detectable abundance of photospheric heavy elements (Chayer et al. 1995). On the other hand, the hydrogen-rich composition of PG 1658+441 is quite interesting. The surface of white dwarfs emerging from the high-end of the main-sequence progenitor mass range (8–10 $M_\odot$) is expected to be depleted of hydrogen and even probably of helium (Garcia-Berro et al. 1997). It may suggest that there was a sufficient amount of hydrogen left deeper in the envelope to form, over time, a hydrogen-dominated atmosphere. On the other hand, the progenitor of PG 1658+441 may have been an early-A or late-B magnetic star which developed a higher degenerate core mass because of the presence of a magnetic field.

Alternatively, the hydrogen-rich atmosphere of PG 1658+441 may suggest that hydrogen was accreted from the interstellar medium as suggested by Segretain et al. (1997). However, in the present case, accretion of interstellar hydrogen may be inhibited by the presence of a magnetic field. Using the formalism of Angel et al. (1981) and assuming that PG 1658+441 is accreting at the Eddington rate as argued by Koester (1976), we calculated that a mean equatorial field of about 4136 G would be sufficient to prevent the accretion flow from reaching the surface of the star (assuming a particle density of 1 cm^{-3} and a velocity of 50 km s^{-1}). With a mean surface field of 2.3 MG (Schmidt et al. 1992), it is unlikely that PG 1658+441 would accrete significantly. Therefore, it is unlikely that the star entered the

white dwarf cooling sequence with an atmosphere devoid of hydrogen.

The detection of quasi-molecular satellite absorption in the Lyman-β and Lyman-γ wings of PG 1658+441 shows that these features can be observed even in hot white dwarfs and that they should be included in the modeling of Lyman lines up to effective temperatures higher than assumed in the past. Our analysis indicates that the treatment of quasi-molecular satellite opacities could be improved, particularly in the range of ionic densities encountered in the atmosphere of ultramassive white dwarfs. Our current approach does indeed have some limitations. For instance, the quasi-molecular satellite profiles we use are based on an expansion in density (Allard et al. 1994) valid for low densities of hydrogen atoms ($n \ll 10^{18}$ cm^{-3}). This approximation is appropriate for white dwarfs with cooler and lower surface gravities but is less acceptable for ultramassive white dwarfs. This might explain in part why the fits shown in previous investigations (Koester et al. 1998; Wolff et al. 2001; Hébrard et al. 2003, for examples) appear somewhat better. Another improvement would be to include a variable dipole moment in the calculations of the satellites of Lyman-γ as suggested by Allard et al. (2003). This may enhance the strength of the Lyman-γ satellites and help improve the fit shown on Fig. 2. At this stage, we have not included the quasi-molecular satellites of the Lyman lines in our model atmosphere calculations because those features are rather weak in comparison with the Stark wings at the relatively high effective temperature of PG 1658+441. In a future investigation, we plan to include the quasi-molecular satellites in the model atmosphere and interpolate in tables of profiles computed for densities appropriate for ultramassive white dwarfs.

In summary, we have presented an analysis of the *FUSE* spectrum of the ultramassive white dwarf PG 1658+441 and we find that:

- The *FUSE* spectra are well represented by a pure hydrogen non-LTE model spectrum computed with the atmospheric parameters determined from optical spectroscopy.
- Lyman-β satellite absorption has been detected at 1058 Å and 1076 Å making PG 1658+441 the hottest star in which these features are detected.
- Upper limits on the abundance of C, N, Si, and P imply that PG 1658+441 has a highly pure hydrogen atmosphere.

This work is based on observations made with the NASA-CNES-CSA Far Ultraviolet Spectroscopic Explorer. *FUSE* is operated for NASA by the Johns Hopkins University under NASA contract NAS5-32985. This research is funded by NASA grants NAG5-11570 and NAG5-11844.

REFERENCES

Achilleos, N. & Wickramasinghe, D. T. 1989, ApJ, 346, 444

Allard, N. F., Kielkopf, J., & Feautrier, N. 1998, A&A, 330, 782

Allard, N. F., Kielkopf, J. F., Hébrard, G., & Peek, J. M. 2003, submitted to European Journal of Physics

Allard, N. F., Koester, D., Feautrier, N., & Spielfiedel, A. 1994, A&AS, 108, 417

Angel, J. R. P., Borra, E. F., & Landstreet, J. D. 1981, ApJS, 45, 457

Barstow, M. A., Good, S. A., Burleigh, M. R., Hubeby, I., Holberg, J. B., & Levan, A. J. 2003, preprint (astro-ph/0306077)

Barstow, M. A., Holberg, J. B., Hubeny, I., Good, S. A., Levan, A. J., & Meru, F. 2001, MNRAS, 328, 211

Chayer, P., Fontaine, G., & Wesemael, F. 1995, ApJS, 99, 189

Dupuis, J., Vennes, S., & Chayer, P. 2002, ApJ, 580, 1091

Finley, D. S., Koester, D., Kruk, J., Kimble, R. A., & Allard, N. F. 1997, in ASSL Vol. 214: White dwarfs, 245

Friedrich, S., Ostreicher, R., & Schweizer, W. 1996, A&A, 309, 227

Garcia-Berro, E., Isern, J., & Hernanz, M. 1997, MNRAS, 289, 973

Green, R. F., Schmidt, M., & Liebert, J. 1986, ApJS, 61, 305

Hébrard, G., Allard, N. F., Hubeny, I., Lacour, S., Ferlet, R., & Vidal-Madjar, A. 2002, A&A, 394, 647

Hébrard, G., Allard, N. F., Kielkopf, J. F., Chayer, P., Dupuis, J., Kruk, J. W., & Hubeny, I. 2003, A&A, 405, 1153

Hubeny, I. 1988, Comput. Phys. Commun., 52, 103

Hubeny, I. & Lanz, T. 1995, ApJ, 439, 875

Koester, D. 1976, A&A, 52, 415

Koester, D., Finley, D. S., Allard, N. F., Kruk, J. W., & Kimble, R. A. 1996, ApJ, 463, L93

Koester, D., Sperhake, U., Allard, N. F., Finley, D. S., & Jordan, S. 1998, A&A, 336, 276

Lemke, M. 1997, A&AS, 122, 285

Liebert, J., Schmidt, G. D., Green, R. F., Stockman, H. S., & McGraw, J. T. 1983, ApJ, 264, 262

Moos, H. W. et al. 2000, ApJ, 538, L1

—. 2002, ApJS, 140, 3

Nomoto, K. 1984, ApJ, 277, 791

Sahnow, D. et al. 2000, ApJ, 538, L7

Schmidt, G. D., Bergeron, P., Liebert, J., & Saffer, R. A. 1992, ApJ, 394, 603

Segretain, L., Chabrier, G., & Mochkovitch, R. 1997, ApJ, 481, 355

Shtol', V. G., Valyavin, G. G., Fabrika, S. N., Bychkov, V. D., & Stolyarov, V. A. 1997, Astronomy Letters, 23, 48

Vennes, S. 1999, ApJ, 525, 995

Vennes, S., Bowyer, S., & Dupuis, J. 1996, ApJ, 461, L103

Weidemann, V. 2000, A&A, 363, 647

Wolff, B., Kruk, J. W., Koester, D., Allard, N. F., Ferlet, R., & Vidal-Madjar, A. 2001, A&A, 373, 674

Table 1. Atmospheric Parameters of PG 1658+441 from *FUSE*

Channel–Segment	$T_{\rm eff}$ ($10^3 K$)	$\log g$ (c.g.s.)	Wavelength Range (Å)
LiF1A	29.4 ± 0.20	9.34 ± 0.15	988–1082
LiF2B	29.7 ± 0.30	9.28 ± 0.20	979–1074
SiC1A	29.4 ± 0.30	9.27 ± 0.20	1004–1090
SiC1B	30.0 ± 0.60	9.31 ± 0.30	905–992
SiC2A	30.9 ± 0.40	9.18 ± 0.32	917–1005
SiC2B	29.3 ± 0.40	9.46 ± 0.34	1017–1104
weighted mean	29.62	9.31	
weighted standard deviation	0.50	0.07	

Table 2. Abundance Upper Limits for PG 1658+441 from *FUSE*

Ionic Species	$\log X/H$
C III	$\lesssim -6.8$
Si III	$\lesssim -7.7$
P IV–P V	$\lesssim -6.0$
N II	$\lesssim -6.5$

Fig. 1.— *FUSE* spectra of PG 1658+441 in the LiF channels. The spectra of PG 1658+441 in the LiF1 and LiF2 channels are dominated by broad Lyman lines. The data are compared to model spectra at $T_{\rm eff} = 30,510$ K and $\log g = 9.36$ including quasi-molecular lines for Lyman-β and Lyman-γ (*dashed line*) and excluding the quasi-molecular lines (*solid line*). The geocoronal H I emission is detected in the core of Lyman-β and Lyman-γ. The emission features in the LiF2A segment are spurious and result from a local degradation of the micro-channel plate gain. Gaps in wavelength coverage are apparent between segments 1A and 1B and between segments 2A and 2B.

Fig. 2.— *FUSE* spectra of PG 1658+441 in the SiC channels. Same as in Figure 1.

Fig. 3.— Fit of the Lyman-β line profile of PG 1658+441 in the LiF1A segment. The upper part of the figure shows a comparison between the LiF1A spectrum (in histogram) and the best fit model (solid line). The fit is restricted to the region delimited by the two vertical dashed lines. The C II and O I features are weak interstellar lines and the absorption line near 1043Å is a spurious feature due to a detector dead spot. In the lower panel, we plot the residuals of the fit which shows significant deviations at the locations of the H_2^+ quasi-molecular satellites of Lyman-β and Lyman-γ. The relatively narrow 1,2, and 3 sigma contours shown in the lower part of the figure indicate that the solution is well constrained.

Fig. 4.— Upper limits on metal abundances in *FUSE* spectrum of PG 1658+441. The non-LTE synthetic spectra of C, N, Si, and P lines are compared to the *FUSE* spectrum. The spectra were computed with abundances set to 3–σ upper limits. The synthetic and observed spectra are plotted as a function of radial velocity centered on the rest wavelength of the line transitions chosen to compute abundance upper limits. The velocity scale is corrected for the predicted gravitational redshift of 211 km s^{-1}.

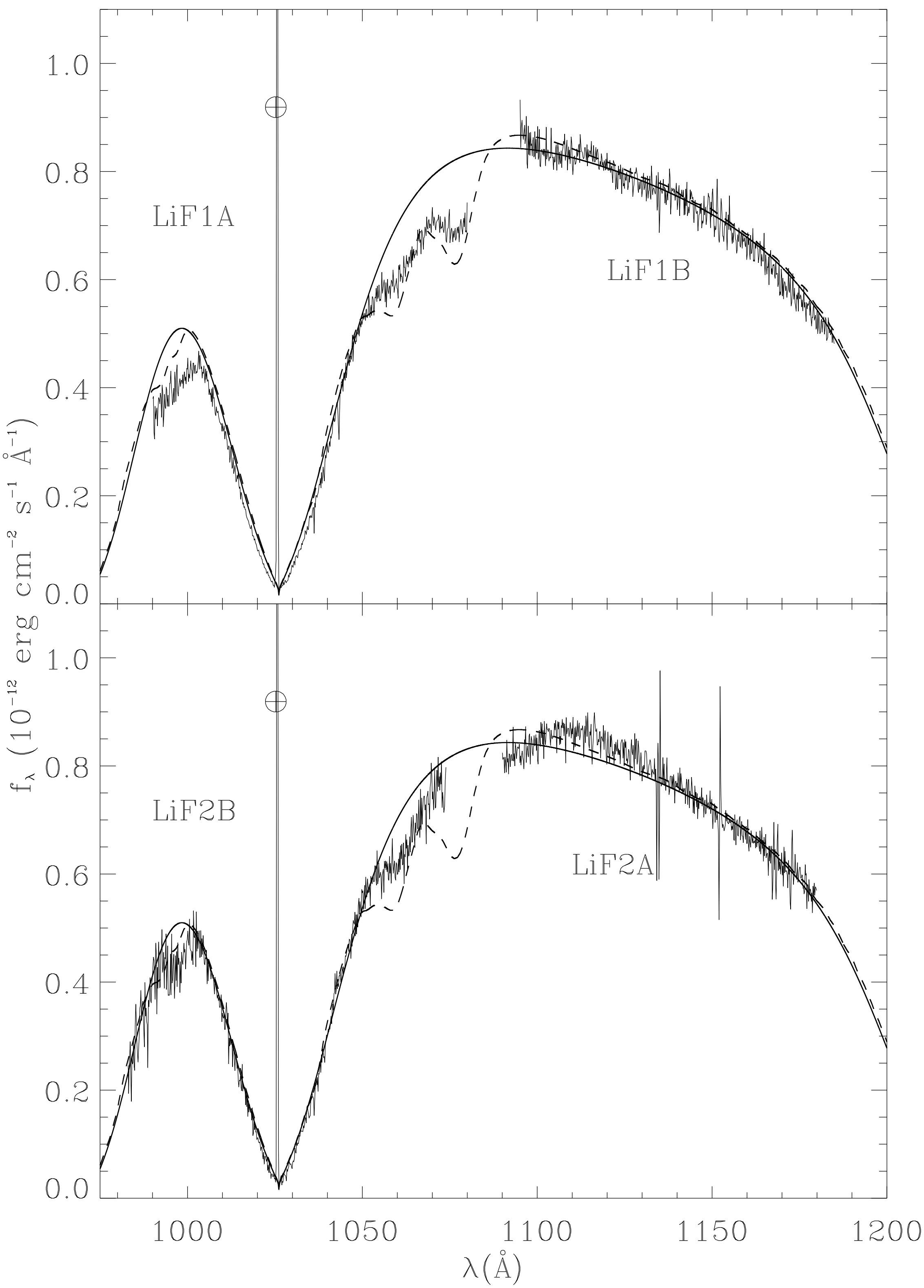

LiF1A
LiF1B
LiF2B
LiF2A
1.0
0.8
0.6
0.4
0.2
0.0
1000
1050
1100
1150
1200
f_λ (10^{-12} erg cm^{-2} s^{-1} Å^{-1})
λ(Å)

Fig. 1.—

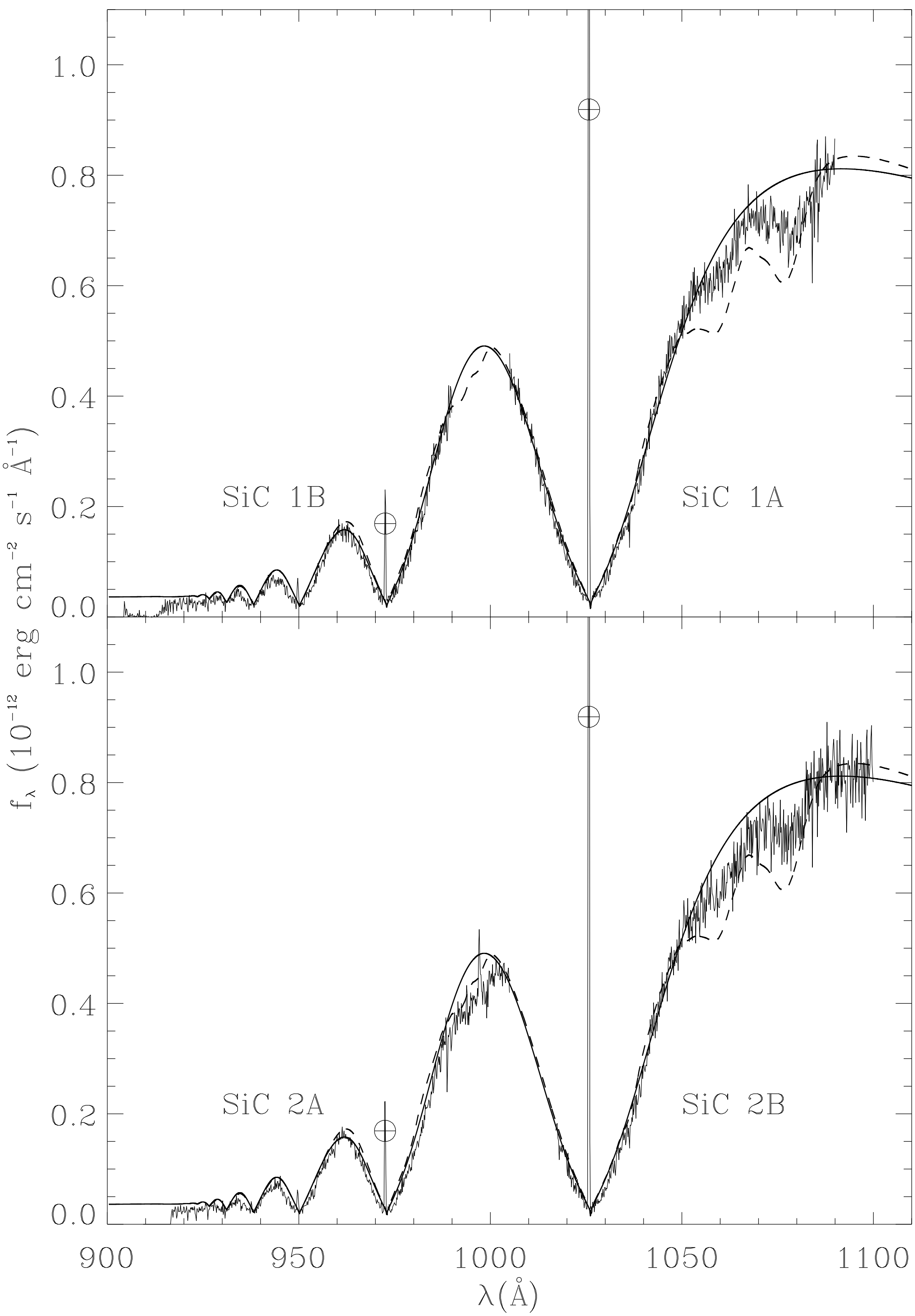
1.0
0.8
0.6
0.4
0.2
0.0
SiC 1B
SiC 1A
SiC 2A
SiC 2B
f_λ (10^{-12} erg cm^{-2} s^{-1} Å^{-1})
900
950
1000
1050
1100
λ(Å)

Fig. 2.—

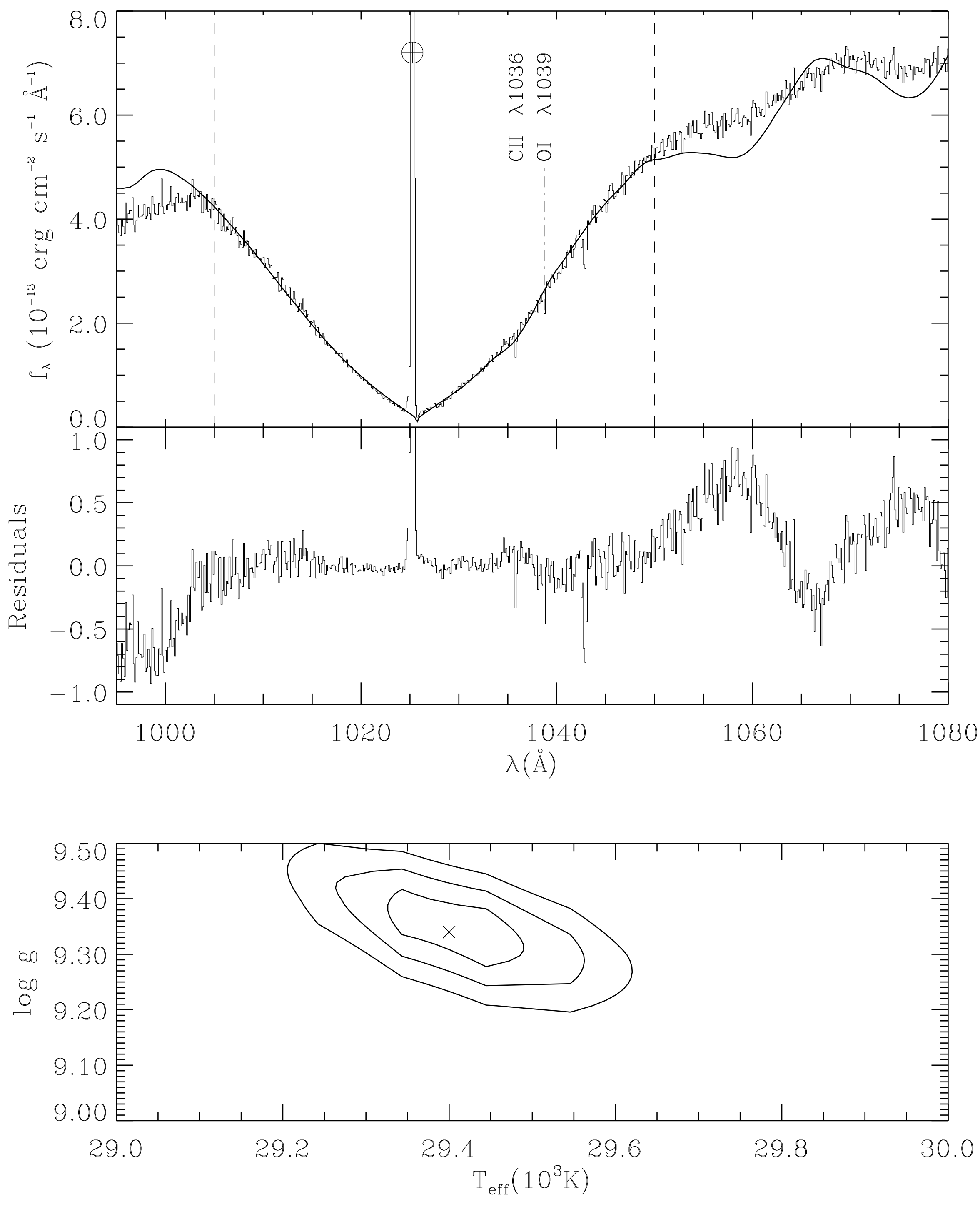
8.0
6.0
4.0
2.0
0.0
f_λ (10^{-13} erg cm^{-2} s^{-1} Å^{-1})
CII λ1036
OI λ1039
1.0
0.5
0.0
−0.5
−1.0
Residuals
1000
1020
1040
1060
1080
λ(Å)
9.50
9.40
9.30
9.20
9.10
9.00
log g
29.0
29.2
29.4
29.6
29.8
30.0
$T_{eff}(10^3K)$

Fig. 3.—

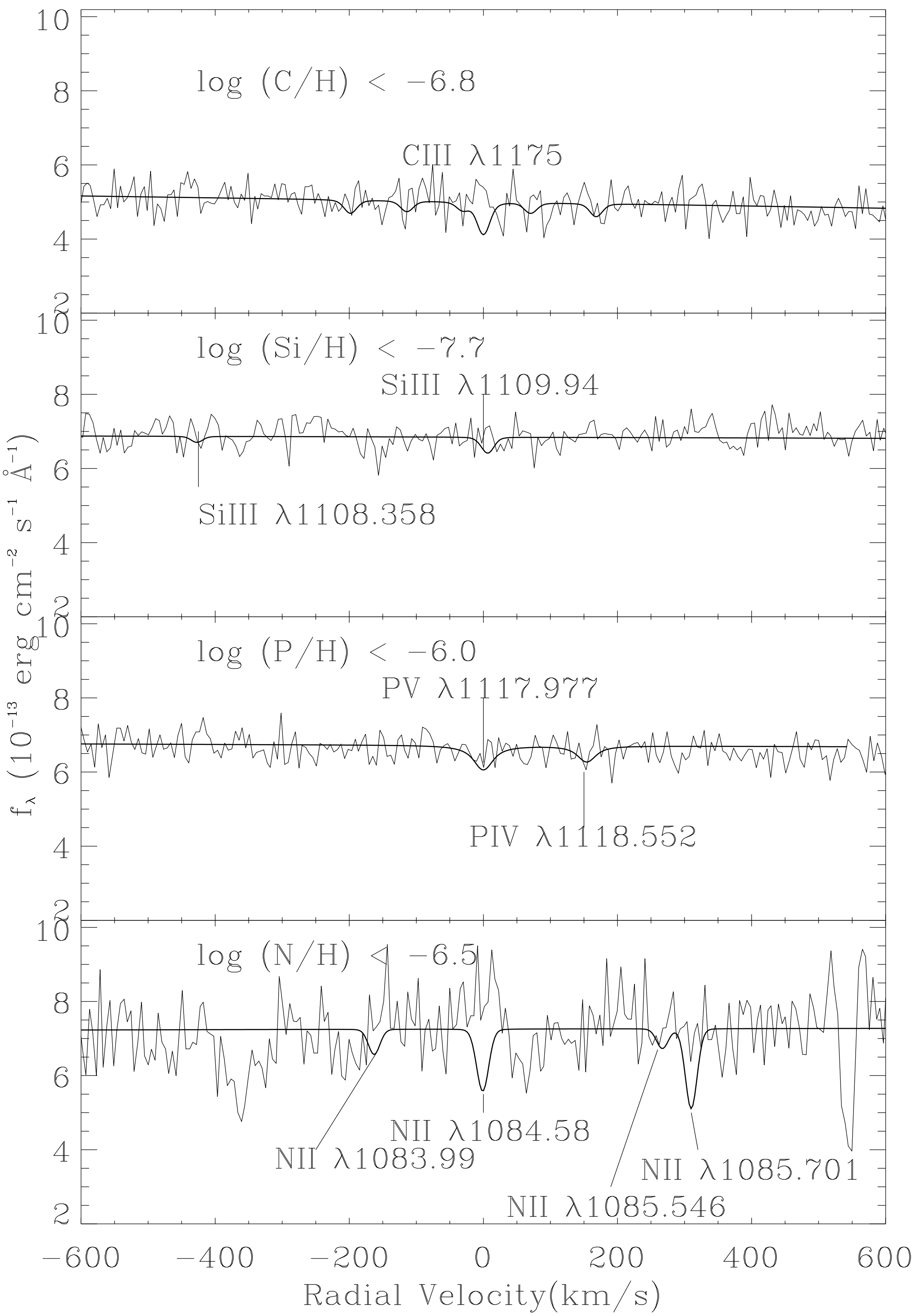
log (C/H) < −6.8
CIII λ1175
log (Si/H) < −7.7
SiIII λ1109.94
SiIII λ1108.358
log (P/H) < −6.0
PV λ1117.977
PIV λ1118.552
log (N/H) < −6.5
NII λ1084.58
NII λ1083.99
NII λ1085.701
NII λ1085.546
f$_\lambda$ (10^{-13} erg cm^{-2} s^{-1} Å^{-1})
Radial Velocity(km/s)
−600
−400
−200
0
200
400
600
2
4
6
8
10

Fig. 4.—